Synthesis of Co_2B Nanostructures and Their Catalytic Properties for Hydrogen Generation

Tuncay Simsek[1], Mustafa Baris[2]

[1]Department of Physics Engineering, Hacettepe University, Ankara, Turkey.
tsimsek@hacettepe.edu.tr
[2]Eti Maden Works General Management, Ankara, Turkey. mustafabaris@etimaden.gov.tr

Corresponding Author: Dr. Tuncay SIMSEK
E-mail: tsimsek@hacettepe.edu.tr
Address: Hacettepe Üniversitesi Beytepe Yerleşkesi, Fizik Mühendisliği Bölümü
06800 - Beytepe Ankara - Türkiye

Abstract

Pure cobalt (II) boride nanoparticles/nanocylinders were synthesized in aqueous media under Argon blanket using cobalt chloride ($CoCl_2$) and sodium borohydride ($NaBH_4$) as reactants. $CoCl_2$ (0.325 g) was dissolved in cold distilled water (DDI) and the solution was introduced into a sealed glass reactor. Then, $NaBH_4$ was then dissolved in DDI (90 mL) and the solution was added drop-wise into the reactor and stirred magnetically at 300 rpm. By the addition of $NaBH_4$ (10 mL, 0.225 g) solution, amorphous black cobalt boride particles were synthesized immediately. The presence of crystalline Co_2B phase with high purity in the nanocylinders which is obtained by calcination at 500°C was shown by X-ray diffraction spectroscopy. An amorphous Co_2B structure was observed with the sample dried under vacuum. In the synthesis runs, Co_2B nanoparticles with different morphological characteristics were achieved by changing the initial $CoCl_2$ concentration and the reaction period. A microscopic structure in the form of nanocylinders was observed for the calcined products. The nanocylinder diameter increased from ca. 30 nm to 100 nm by increasing the reaction time from 3 to 120 min. $CoCl_2$ initial concentration was also found another factor increasing the nanocylinder diameter. The nanocylinders with diameters between 80-500 nm were obtained by increasing $CoCl_2$ concentration from 12.6 to 100.1 mM. The lowest and highest saturation magnetization values were obtained 19 and 69 emu/g for crystalline sample calcined under air (Co-Co_2B mixture) and amorphous Co_2B sample obtained by vacuum-drying, respectively. Amorphous and crystalline Co_2B samples were used as catalyst for Hydrogen generation by the hydrolysis of $NaBH_4$ in aqueous media. Amorphous Co_2B gave significantly higher H_2 generation rate with respect to the catalysts prepared by calcination of amorphous Co_2B under air or Argon at 500°C. The maximum H_2 generation rate was obtained as 1.1 L/g catalyst.min by using amorphous Co_2B with 1 % w/w of initial $NaBH_4$ concentration.

Key words: Cobalt boride, H_2 generation, sodium borohydride, hydrolysis, cobalt oxide.

1. Introduction

Significant attention was paid on H_2 carriers due to the difficulties appeared in the storage and transport of H_2. The non-toxic character of H_2, the flexibility of source materials used for generation, low-cost production and taking place of the source reaction at ambient conditions are known as the basic advantages of the H_2 energy. Although various methods have been proposed for H_2 generation, the hydrolysis of alkali metal hydrides is mostly preferred as a favorable method. Among these materials, sodium borohydride is the most widely used

reactant for H_2 generation due to its high H_2 content (10.7 % w/w). All of H_2 content of $NaBH_4$ have been recovered by using appropriate catalysts in aqueous media. Various types of catalysts have been tried for H_2 generation by the hydrolysis of $NaBH_4$ in aqueous-alkaline media [1-43]. Generally, transition metal based catalysts are preferred. Cobalt (II) salts were tried as catalyst for generating H_2 from sodium borohydride [1]. On the other hand, various catalysts based on supported cobalt were also tried [2-11].

Metal borides synthesized via mechanochemical, borothermal or carbothermal route, electrolysis in a fused salt, chemical vapor deposition or carbothermal method are another group of materials widely used for H_2 generation by the decomposition of $NaBH_4$ [12-14]. On the other hand, the catalysts including the alloys of metal borides were recently tried for obtaining higher H_2 generation rates in the decomposition of $NaBH_4$ [15-24].

There have been numerous studies in the literature on the H_2 generation by using cobalt boride as catalyst in the decomposition of $NaBH_4$ [25-33]. In most of these studies, the crystalline phases containing either –various- cobalt borides or metallic cobalt in the form of irregular nanoparticles were tested as catalyst for H_2 production. In our study, both the synthesis of cobalt boride and the drying and calcination of cobalt boride product were carried out under Ar atmosphere. Hence both the synthesis and calcination conditions were carefully controlled. Then amorphous Co_2B or crystalline pure Co_2B phases were obtained in the form of nanocylinders by a modified form of solvothermal method based on the chemical reaction between cobalt chloride and sodium borohydride. Here, we wish to report their properties and catalytic performance of pure amorphous/crystalline Co_2B in H_2 generation by the decomposition of $NaBH_4$.

2. Experimental

2.1. Materials

Cobalt chloride ($CoCl_2$), sodium borohydride ($NaBH_4$) were supplied from Aldrich Chem. Corp., U.S.A. and used as received. The synthesis reactions were conducted under high purity of Ar atmosphere (Habaş, Turkey). Distilled-deionized water was used in all experiments.

2.2. Synthesis of Co_2B particles

The synthesis of cobalt boride (Co_2B) nanoparticles was performed in an aqueous medium. In the synthesis runs, $CoCl_2$ concentration in the initial reaction medium and the reaction period were changed. Typically, $CoCl_2$ (0.325 g) was dissolved in cold DDI water (90 mL) and the solution was introduced into a sealed, three-necked glass reactor stirred magnetically at 300 rpm, placed in an ice-bath kept at +4ºC. Then, the flow of Ar into the reactor was initiated. The reactor was stirred for 10 min for thermal equilibrium. $NaBH_4$ was then dissolved in DDI water (10 mL) and the solution was added drop-wise into the reactor within 3 min. By the addition of $NaBH_4$ solution (10 mL, 0.225 g), the reaction medium turned to black. The reaction was continued under Ar atmosphere to prevent oxidation. The black cobalt boride particles were synthesized immediately. Following to the completion of reaction-period selected, the reaction medium was filtrated under Ar-protection. The black cake was extensively washed with DDI water under Ar atmosphere. The nanoparticles isolated were dried in vacuo at 70 ºC for 24 h. Dry cobalt boride powder was calcined at 500ºC for 2 hours, under Ar atmosphere with a heating rate of 2 ºC/min.

2.3. Characterization of Co_2B particles

The crystal structure was analysed by X-ray diffraction spectrophotometer (Rigaku, D/MAX-2200) for both dried and calcined Co_2B nanoparticles. The particle morphology was determined by Scanning Electron Microscopy (FEI, Quanta 200F, U.S.A.). The magnetic properties of Co_2B nanoparticles were determined by Vibrating Sample Magnetometer (PPMS, P525, U.S.A.). The specific surface area was measured by a surface area and pore-size analyzer (Quantaochrome, Nova 220E, U.S.A.) using nitrogen adsorption-desorption method together with Brunauer-Emmett-Teller (BET) equation.

2.4. H_2 generation using Co_2B nanoparticles as catalyst

H_2 generation runs by the hydrolysis of $NaBH_4$ were conducted in a pyrex glass reactor equipped with an apparatus capable of measuring the H_2 evolved according to the water-displacement method (Figure 1). Two separate sets of H_2 generation runs were performed by using the calcined Co_2B samples obtained with different $CoCl_2$ initial concentrations and different reaction periods, respectively. A third set of runs for H_2 generation were also performed by using the amorphous Co_2B obtained by vacuum-driying of reaction product at 70ºC, the crystalline Co_2B obtained by calcining the reaction product under Ar at 500ºC and the crystalline Co_2B-Co mixture obtained by calcining the reaction product under air at 500ºC as catalysts.

Figure 1. H_2 generation measuring apparatus

Typically, the solution (10 mL) DDI and $NaBH_4$ (1 % w/w) were prepared. Then, CoB_2 catalyst (0.1 g) was added into the solution under magnetic stirring at 300 rpm. The valve on the line passing to the displacement tube was opened. The volume of H_2 generated was measured by water-displacement method with the progressing hydrolysis.

3. Result and Discussion

3.1. Characterization of Co_2B nanostructures

Cobalt boride particles were obtained by the reaction of $CoCl_2$ with $NaBH_4$ in the aqueous media kept at +4ºC, under Ar atmosphere according to the following equation [44].

$$2CoCl_2 + 4NaBH_4 + 9H_2O \longrightarrow Co_2B + 4NaCl + 12.5H_2 + 3B(OH)_3 \qquad (1)$$

Equation 1 shows the reduction reaction of $CoCl_2$ with effective reducing agent $NaBH_4$. During the reduction, while Co ions reacts rapidly with boron to form Co_2B nanoparticles, as a by-product, NaCl and H_3BO_3 compounds were formed and H_2 gas was released. The synthesized Co_2B particle size distributions were in the range of nano-size due to the fast reaction but also high surface energy causes to agglomeration due to the non-crystalline structure of particles [17, 26, 30]. SEM images and XRD patterns of the powders obtained after the synthesis experiments according to the reactions in Equation 1 and the powders calcined under Ar atmosphere and air are given in Figure 2. The Figure shows that the black powders obtained after synthesis experiments have amorphous structure and composed of irregular nanoparticles ranging from 10 to 300 nm. The calcined powder under air conditions at 500 ºC was found to consist of Co-Co_2B fingertype structured particles ranging from 50-

300 nm. Calcining the powders under the Ar atmosphere at the same temperature resulted in fingertype pure Co_2B of 50-100 nm size. The specific surface areas (SSA) were determined as 10.0, 6.0 and 3.0 m^2/g for the amorphous Co_2B, Co_2B calcined under Ar and Co_2B calcined under air, respectively. Wu et al. have calcined the powders they synthesized in a similar study under vacuum at 90-300-500-700 °C. They reported that the structure at 90 °C was amorphous while the structures at 300 and 500 °C consisted of Co-Co_2B and the structure at 700 °C was composed of metallic Co [25]. In another similar study conducted by Jeong et al., it is reported that powders produced were calcined at 500 °C under 1% air-mixed N_2 gas atmospheres were composed of mainly by Co_3O_4 phase and some CoB, Co_2B, Co_3B phases [28].

Figure 2. X-Ray diffraction spectra and SEM images of amorphous Co_2B (a), crystalline Co-Co_2B calcined under air (b), crystalline Co_2B calcined under Ar (c).

Pure Co_2B synthesis experiments were performed in two sets, and the effect of reaction time and $CoCl_2$ concentration on the morphology of nanoparticles was investigated. In the first set of the synthesis runs, the reaction time was changed by keeping the other conditions as constant. The SEM images and X-ray diffraction spectra of Co_2B particles obtained with different reaction periods and calcined under Ar at 500°C are given in Figure 3. As seen here, Co_2B particles in the form of nanocylinders were observed. Both the diameter and the length of the nanocylinders increased with increasing reaction period. The aspect ratio of the nanocylinders roughly changed from 2.3 to 4.0 by increasing reaction period from 3 to 120 min (i.e. determined by SEM photos in Figure 3).

Figure 3. SEM images and X-ray diffraction spectra of cobalt boride particles obtained with different reaction times. (Reaction time (min): (a) 3, (b) 12, (c) 60, (d) 120; $CoCl_2$ concentration:25.0 mM; $NaBH_4$ concentration:59.50 mM, Temperature: +4°C; Stirring rate:400 rpm; Ar atmosphere)

X-ray diffraction spectra of Co_2B particles obtained with different reaction periods and calcined under Ar at 500 °C are given in Figure 3, only the peaks specific to the crystalline Co_2B phase were observed in the spectra obtained with the nanocylinders synthesized with the reaction periods of 12, 60 and 120 min. The peaks belonging to minor impurities were detected at 50-54 degrees in the spectrum belonging to the nanocylinder sample obtained with the shortest reaction period (i.e. 3 min).

Figure 4. SEM images and X-ray diffraction spectra of cobalt boride particles obtained with different $CoCl_2$ initial concentrations. ($CoCl_2$ concentration (mM): (a) 12.6, (b) 25.0, (c) 50.1 (d) 100.1, $NaBH_4/CoCl_2$ molar ratio: 2.4, Reaction time: 12 min, Temperature: +4°C, Stirring rate: 400 rpm, Ar atmosphere.)

The SEM images and X-ray diffraction spectra of Co_2B particles obtained with different $CoCl_2$ initial concentrations and calcined under Ar at 500°C are given in Figure 4. As seen here, the size of nanocylinders markedly increased with the increasing $CoCl_2$ initial concentration. XRD spectra exhibited the peaks specific to the crystalline Co_2B phase for all $CoCl_2$ initial concentrations. From the SEM images, it can be seen that the smallest grain size was obtained at the concentration of 25.0 mM $CaCl_2$, about 80-100 nm. It was found that the fingertype structure was irregularly shaped with a size of about 500 nm by increasing the concentration.

The magnetization curves of the amorphous and crystalline Co_2B nanocylinders are given in Figure 5. As seen here, all samples exhibited ferromagnetic behavior. The highest saturation magnetization was observed with the Co-Co_2B sample calcined under air. XRD examination of this sample showed the presence of metallic Co phase after calcination under air (as will be seen in Figure 2b). The saturation magnetization values were measured as 19.0, 44.0 and 68.5 emu/g for the amorphous and crystalline Co_2B samples calcined under Ar and air, respectively (Figure 5). We have obtained similar results in another study of the production of Co_2B nanocrystals by mechanochemical method. It was determined that pure Co_2B nanocrystals showed ferromagnetic characteristics with a saturation magnetization changing between 38-48 emu/g [45].

Figure 5. Magnetization curves of the cobalt boride nanoparticles calcined under different conditions

3.2. H_2 generation runs

In the H_2 generation runs, the effect of calcination conditions on the catalytic activity of Co_2B samples was tested. The variation of H_2 volume with the time by using amorphous and crystalline Co_2B samples is given in Figure 6. The H_2 generation rates achieved with amorphous and crystalline Co_2B catalysts with the initial $NaBH_4$ concentration of 1 % w/w are given in Table 1 (Runs C1, C2 and A1). As seen here, the highest H_2 generation rate was obtained with the amorphous Co_2B obtained by drying the reaction product at 70^oC in vacuo. The crystalline Co_2B samples obtained by the calcination of reaction product (under Ar or air) gave lower H_2 generation rates with respect to the amorphous one. Note that the lowest H_2 generation rate was obtained with the Co_2B sample obtained by calcination in air (Figure 6 and Table 1). The H_2 generation rates found with amorphous and calcined Co_2B samples obeyed the order observed for SSA (Table 1). Note that, higher H_2 generation rates were also reported for the amorphous Co_2B samples with respect to the crystalline ones [26, 27, 30, 31].

Figure 6. The variation of hydrogen volume with the time by using cobalt boride nanoparticles/nanocylinders obtained with different calcination conditions as catalyst in the hydrolysis of $NaBH_4$. Co_2B concentration: 10 mg/mL, Initial $NaBH_4$ concentration: 263.1 mM (~1 % w/w), NaOH concentration: 250 mM, Room temperature.

Table 1. Hydrogen generation rates obtained with the crystalline and amorphous Co_2B samples at different conditions.

The effects of the synthesis parameters on H_2 production were examined. The H_2 production of the amorphous powders obtained by changing the reaction time and the $CoCl_2$ concentration were found to be close to each other. The highest H_2 generation rate was calculated as 1110 mL H_2/min. g catalyst by using the initial slope of the curve obtained with the Co_2B sample produced with the reaction period of 12 min (Table 1). Co_2B samples with other reaction periods gave lower H_2 generation rates. For the amorphous Co_2B samples produced with different $CoCl_2$ initial concentrations, the variation of volume of H_2 generated with the time was also determined. However, no significant effect of $CoCl_2$ initial concentration used in the synthesis of Co_2B was observed on the H_2 generation rate.

A separate set of H_2 generation runs was performed to determine the effects of catalyst (Co_2B) concentration and initial $NaBH_4$ concentration the H_2 generation rate. The variation of H_2

volume with the time for different catalyst (amorphous Co_2B) and initial $NaBH_4$ concentrations is given in Figure 7. The H_2 generation rates calculated from the curves in Figure 7 are given in Table 1.

Figure 7. The variation of H_2 volume with the time by using different concentrations of cobalt boride nanoparticles/nanocylinders and different initial $NaBH_4$ concentrations in the hydrolysis of $NaBH_4$. NaOH concentration: 250 mM, Room temperature.

As seen from Figure, the H_2 generation rate exhibited a decrease with decreasing catalyst concentration (Experiments A1, A2 and A3 in Table 1). In order to test the effect of initial $NaBH_4$ concentration on the H_2 generation rate, the initial $NaBH_4$ concentration was changed in three levels (i.e. 1, 10 and 20 % w/w). In this set, the catalyst (amorphous Co_2B) concentration was kept constant at 1 mg/mL (Experiments A3, A4 and A5 in Table 1). The H_2 generation curves obtained with the initial $NaBH_4$ concentrations of 1 and 10 % w/w are also shown in Figure 7. As seen here, the H_2 generation rates obtained with the $NaBH_4$ concentrations of 1 and 10 % w/w were almost the same. As seen in Table 1, no significant change in the H_2 generation rate was observed when $NaBH_4$ concentration was changed between 1-20 % w/w (Experiments A3, A4 and A5). Nearly zeroth order rate behavior with respect to initial $NaBH_4$ concentration was observed in the presence of Co_2B catalysts as also reported elsewhere [26, 31].

Table 2. The properties of hydrogen generation rates of catalysts containing Co_2B phase

The comparison of maximum H_2 generation rate achieved in our study with the Co_2B based catalysts produced in the previous studies is given in Table 2. As seen here, the maximum H_2 generation rate observed in our study was lower with respect to those obtained with the similar Co_2B containing catalysts. This should be related to lower specific surface area of the amorphous Co_2B catalyst synthesized in our study (i.e. 10 m^2/g). In the studies included in Table 2, relatively higher H_2 generation rates were obtained by using porous catalysts containing Co_2B with the SSA values ranging between 30-114 m^2/g [25, 27, 28, 30, 31]. On the other hand, the H_2 generation rate based on surface area was also calculated by considering the specific surface area values of the catalysts listed in Table 2. When the H_2 generation rate based on surface area is considered, one can conclude that, amorphous Co_2B nanoparticles synthesized in our case exhibited a satisfactory catalytic performance with respect to the similar catalytic materials listed in Table 2. The synthesis conditions providing amorphous-pure Co_2B in the porous form with high specific surface area are still under investigation.

4. Conclusion

Cobalt (II) boride nanoparticles/nanocylinders with high purity were synthesized. The synthesized powders were amorphous and composed of irregular nanoparticles ranging from 10 to 300 nm. The calcined powder under air conditions at 500 ^oC was found to be consist of Co-Co_2B fingertype structured particles ranging from 50-300 nm while calcining the powders under the Ar atmosphere at the same temperature resulted in fingertype pure Co_2B of 50-100 nm size. Nanocylinder diameter increased from 30 to 100 nm by increasing reaction time. The saturation magnetization values were measured as 19.0, 44.0 and 68.5 emu/g for the amorphous and crystalline Co_2B samples calcined under Ar and air respectively while the specific surface areas (SSA) were determined as 10.0, 6.0 and 3.0 m^2/g for the amorphous Co_2B, Co_2B calcined under Ar and Co_2B calcined under air, respectively. Co_2B

nanoparticles/nanocylinders were used as catalyst for H_2 generation. The highest H_2 generation rate was calculated as 1110 mL H_2/min. g catalyst by using the initial slope of the curve obtained with the Co_2B sample produced with the reaction period of 12 min Amorphous Co_2B gave higher H_2 generation rate than crystalline samples and H_2 generation rate based on surface area was very close to similar catalysts.

Acknowledgements

The authors are very grateful to Eti Maden Works General Management for financial support and laboratory facilities usage.

The authors declare that there are no conflicts of interest.

References

[1] Akdim, A., Demirci U., Muller D., Miele P., Cobalt (II) salts, performing materials for generating hydrogen from sodium borohydride, Int. J. Hydrogen Energy, 34, 2631-2637, 2009.

[2] Zhao J., Ma H., Chen J., Improved hydrogen generation from alkaline $NaBH_4$ solution using carbon-supported Co-B as catalysts, Int. J. Hydrogen Energy, 32, 4711-4716, 2007.

[3] Ye W., Zhang H., Xu D., Ma L., Yi B., Hydrogen generation utilizing alkaline sodium borohydride solution and supported cobalt catalyst, J. Power Sources, 164, 544-548, 2007.

[4] Xu D., Dai P., Liu X., Cao C., Guo Q., Carbon-supported cobalt catalyst for hydrogen generation from alkaline sodium borohydride solution, J. Power Sources, 182, 616-620, 2008.

[5] Lin SSY., Kim D.H., Ha S.Y., Hydrogen production from ethanol steam reforming over supported cobalt catalysts, Catal. Lett., 122, 295-301, 2008.

[6] Dai HB., Liang Y., Wang P., Yao X., Rufford T., Lu M., Cheng H., High-performance cobalt–tungsten–boron catalyst supported on Ni foam for hydrogen generation from alkaline sodium borohydride solution, Int. J. Hydrogen Energy, 33, 4405-4412, 2008.

[7] Hung T.F., Kuo H.C., Tsai C.W., Chen H.M., Liu R.S., Bing-Jhih Weng B.J., Lee J.F., An alternative cobalt oxide-supported platinum catalyst for efficient hydrolysis of sodium borohydride, J. Mater. Chem., 21, 11754-11759. 2011.

[8] Shubhanwita S., Abhirup B., Debnath D., Saibal G., Dipali B., Kajari K., Novel graphene supported Co rich connected core(Pt)-shell(Co) nano-alloy catalyst for improved hydrogen generation and electro-oxidation, Int. J. Hydrogen Energy, 41, (41), 18451–18464, 2016.

[9] Yuyao H., Kunyang W., Liang C., Wenxin Z., Abdullah M.A., Xuping S., Effective hydrolysis of sodium borohydride driven by self-supported cobalt oxide nanorod array for on-demand hydrogen generation, Catal. Commun., 87, 94–97, 2016.

[10] Netskina O.V., Komova O.V., Simagina V.I., Odegova G.V., Prosvirin I.P., Bulavchenko O.A., Aqueous-alkaline $NaBH_4$ solution: The influence of storage duration of solutions on reduction and activity of cobalt catalysts, Renewable Energy, 99, 1073–1081, 2016.

[11] Murat Bilen M., Yılmaz O., Gürü M., Synthesis of $LiBH_4$ from $LiBO_2$ as hydrogen carrier and its catalytic dehydrogenation, Int. J. Hydrogen Energy, 40 (44), 15213-15217, 2015.

[12] Walter JC., Zurawski A., Montgomery D., Thornburg M., Revankar S., Sodium borohydride hydrolysis kinetics comparison for nickel, cobalt, and ruthenium boride catalysts, J. Power Sources,179, 335-339, 2008.

[13] Hua D., Hanxi Y., Xinping A., Chuansin C., Hydrogen production from catalytic hydrolysis of sodium borohydride solution using nickel boride catalyst, Int. J. Hydrogen Energy, 28, 1095-1100, 2003.

[14] Liu BH., Li ZP., Suda S., Nickel and cobalt-based catalysts for hydrogen generation by hydrolysis of borohydride, J. Alloys Compd., 415, 288-293, 2006.

[15] Soler L., Macanás J., Muñoz M., Casado J., Synergistic hydrogen generation from aluminum, aluminum alloys and sodium borohydride in aqueous solutions, Int. J. Hydrogen Energy, 32, 4702-4710, 2007.

[16] Park JH., Shakkthivel P., Kim HJ.,. Han MK, Jang JH., Kim YR, Kim HS., Shul YG., Investigation of metal alloy catalyst for hydrogen release from sodium borohydride for polymer electrolyte membrane fuel cell application, Int. J. Hydrogen Energy, 33, 1845-1852, 2008.

[17] Fernandes R., Patel N., Miotello A., Efficient catalytic properties of Co–Ni–P–B catalyst powders for hydrogen generation by hydrolysis of alkaline solution of $NaBH_4$, Int. J. Hydrogen Energy, 34, 2893-2900, 2009.

[18] Patel N., Patton B., Zanchetta C., Fernandes R., Guella G., Kale A., Miotello A., Pd-C powder and thin film catalysts for hydrogen production by hydrolysis of sodium borohydride, Int. J. Hydrogen Energy, 33, 287-292, 2008.

[19] Patel N., Fernandes R., Miotello A., Promoting effect of transition metal-doped Co–B alloy catalysts for hydrogen production by hydrolysis of alkaline $NaBH_4$ solution, J. Catal., 271,315-324, 2010.

[20] Ding XL., Yuan X., Jia C., Ma ZF., Hydrogen generation from catalytic hydrolysis of sodium borohydride solution using Cobalt-Copper-Boride (Co-Cu-B) catalysts, Int. J. Hydrogen Energy, 35 (20), 11077-11084, 2010.

[21] Patel N., Guella G., Kale A., Miotello A., Patton B., Zanchetta C., Mirenghi L., Rotolo P., Thin films of Co–B prepared by pulsed laser deposition as efficient catalysts in hydrogen producing reactions, Appl. Catal., A, 323, 18-24, 2007.

[22] Yan W, Yunshu L., Dan W., Shiwei W., Zhongqiu C., Ke Z., Hongxin L., Shigang X., Hydrogen generation from hydrolysis of sodium borohydride using nanostructured Ni-B catalysts, Int. J. Hydrogen Energy, 41 (36), 16077–16086, 2016.

[23] Zhihua L., Qiming L., Fang L., Shiduo Z., Xin X., Hydrogen generation from hydrolysis of $NaBH_4$ based on high stable $NiB/NiFe_2O_4$ catalyst, Int. J. Hydrogen Energy, 2016, http://dx.doi.org/10.1016/j.ijhydene.2016.10.115.

[24] Zhenkai C., Yueping G., Jiantai M., In situ synthesis of graphene supported Co-Sn-B alloy as an efficient catalyst for hydrogen generation from sodium borohydride hydrolysis, Int. J. Hydrogen Energy, 41 (3), 1592–1599, 2016.

[25] Wu C., Wu F., Bai Y., Yi B., Zhang H., Cobalt boride catalysts for hydrogen generation from alkaline $NaBH_4$ solution, Mater. Lett., 59, 1748-1751, 2005.

[26] Jeong S., Kim R., Cho E., Kim HJ., Nam SW., Oh IH., Hong SA., Kim S., A study on hydrogen generation from $NaBH_4$ solution using the high-performance Co-B catalyst, J. Power Sources, 144, 129-134, 2005.

[27] Lee J., Kong KY., Jung CR., Cho E., Yoon SP., Han J., Lee TG., Nam SW., A structured Co–B catalyst for hydrogen extraction from $NaBH_4$ solution, Catal. Today, 120, 305-310, 2007.

[28] Jeong S., Cho E., Nam SW., Oh IH., Jung U., Kim S., Effect of preparation method on Co–B catalytic activity for hydrogen generation from alkali $NaBH_4$, Int. J. Hydrogen Energy, 32, 1749-1754, 2007.

[29] Arzac G.M., Rojas T.C., Fernandez A., Boron Compounds as Stabilizers of a Complex Microstructure in a Co-B-based Catalyst for $NaBH_4$ Hydrolysis, ChemCatChem, 3 (8), 1305-1313, 2011.

[30] Xiaochen S., Min D., Ming G., Bin Z., Weiping D., Solvent effects in the synthesis of CoB catalysts on hydrogen generation from hydrolysis of sodium borohydride, Chin. J. Catal., 34, 979-985, 2013.

[31] Gupta S., Patel N., Fernandes R., Kothari D., Miotello A., Mesoporous Co-B nanocatalyst for efficient hydrogen production by hydrolysis of sodium borohydride, Int. J. Hydrogen Energy, 38, 14685-14692, 2013.

[32] Netskina O.V., Ozerova A.M., Komova O.V., Odegova G.V., Simagina V.I., Hydrogen storage systems based on solid-state $NaBH_4/Co_xB$ composite: Influence of catalyst properties on hydrogen generation rate, Catal. Today, 245, 86–92, 2015.

[33] Paladini M., Godinho V., Arzac G.M., Jiménez de Haro M.C., Beltrán A.M., Fernández A., Tailor-made preparation of Co–C, Co–B, and Co catalytic thin films using magnetron sputtering: insights into structure–composition and activation effects for catalyzed $NaBH_4$ hydrolysis, RSC Adv., 6, 108611-108620, 2016.

[34] Nurettin S., Fahriye S., A facile synthesis route to improve the catalytic activity of inherently cationic and magnetic catalyst systems for hydrogen generation from sodium borohydride hydrolysis, Fuel Process. Technol., 132, 1–8, 2015.

[35] Ömer Ş., M. Sait İ., Erhan O., Cafer S., Influence of the using of methanol instead of water in the preparation of $Co–B–TiO_2$ catalyst for hydrogen production by $NaBH_4$ hydrolysis

and plasma treatment effect on the Co–B–TiO_2 catalyst, Int. J. Hydrogen Energy, 41 (4), 2539–2546, 2016.

[36] Kun-Yi A.L., Hsuan-Ang C., Efficient hydrogen production from $NaBH_4$ hydrolysis catalyzed by a magnetic cobalt/carbon composite derived from a zeolitic imidazolate framework, Chemical Engineering Journal, 296, 243–251, 2016.

[37] Yueping G., Gongxuan L., Graphene supported Co–Mo–P catalyst for efficient photocatalyzed hydrogen generation, Int. J. Hydrogen Energy, 41 (16), 6706–6712, 2016.

[38] Ömer Ş., Dilek K., Cafer S., Hydrogen generation from hydrolysis of sodium borohydride with a novel palladium metal complex catalyst, J. Energy Inst., 89 (2), 182–189, 2016.

[39] Yang X.J., Li L.L., Sang W.L., Zhao J.L., Wang X.X., Yu C., Zhang X.H., Tang C.C., Boron nitride supported Ni nanoparticles as catalysts for hydrogen generation from hydrolysis of ammonia borane, J. Alloys Compd., 693, 642–649, 2017.

[40] Özsaçmacı G., Çetin Çakanyıldırım Ç., Gürü M., Co-Mn/TiO_2 catalyst to enhance the $NaBH_4$ decomposition, Journal of Boron, 1 (1), 1-5, 2016.

[41] Braga A.H., Sodre E.R., Santos J.B.O., Marques C.M.P., Bueno J.M.C., Steam reforming of acetone over Ni- and Co-based catalysts: Effect of the composition of reactants and catalysts on reaction pathways, Nanotechnology, 27 (46), 2016.

[42] Nandi D.K., Manna J., Dhara A., Sharma P., Sarkar S.K., Atomic layer deposited cobalt oxide: An efficient catalyst for NaBH4 hydrolysis, J. Vac. Sci. Technol. A, 34, 01A115, 2016.

[43] Chang J., Song W., Li T., Chen J., Wu H., Li C., Fan M., Accelerated Hydrolysis of Solid-state NaBH4/Al System by Co2B Milled with Li for Hydrogen Generation., J. New Mater. Electrochem. Syst, 19 (2), 109-115, 2016.

[44] G.N. Glavee, K.J. Klabunde, C.M. Sorensen, G.C. Hadjipanayis, Langmuir, 9, 162-169 (1993).

[45] Baris M., Simsek T., Akkurt A., Mechanochemical Synthesis and Characterization of Pure Co_2B Nanocrystals, Bull. Mater. Sci., 39 (4), 1119-1126, 2016.

Figures

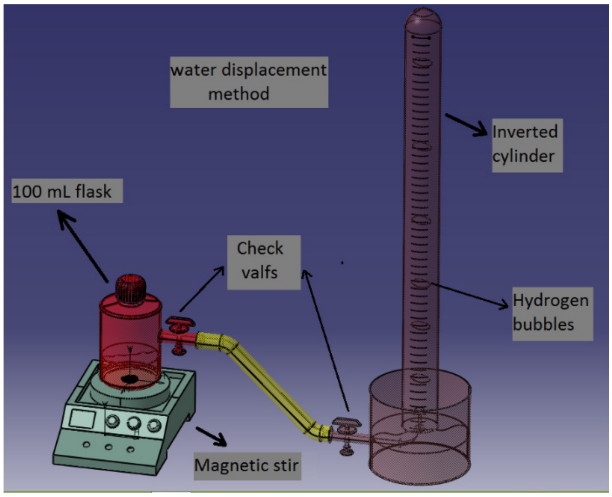

Figure 1. H_2 generation measuring apparatus

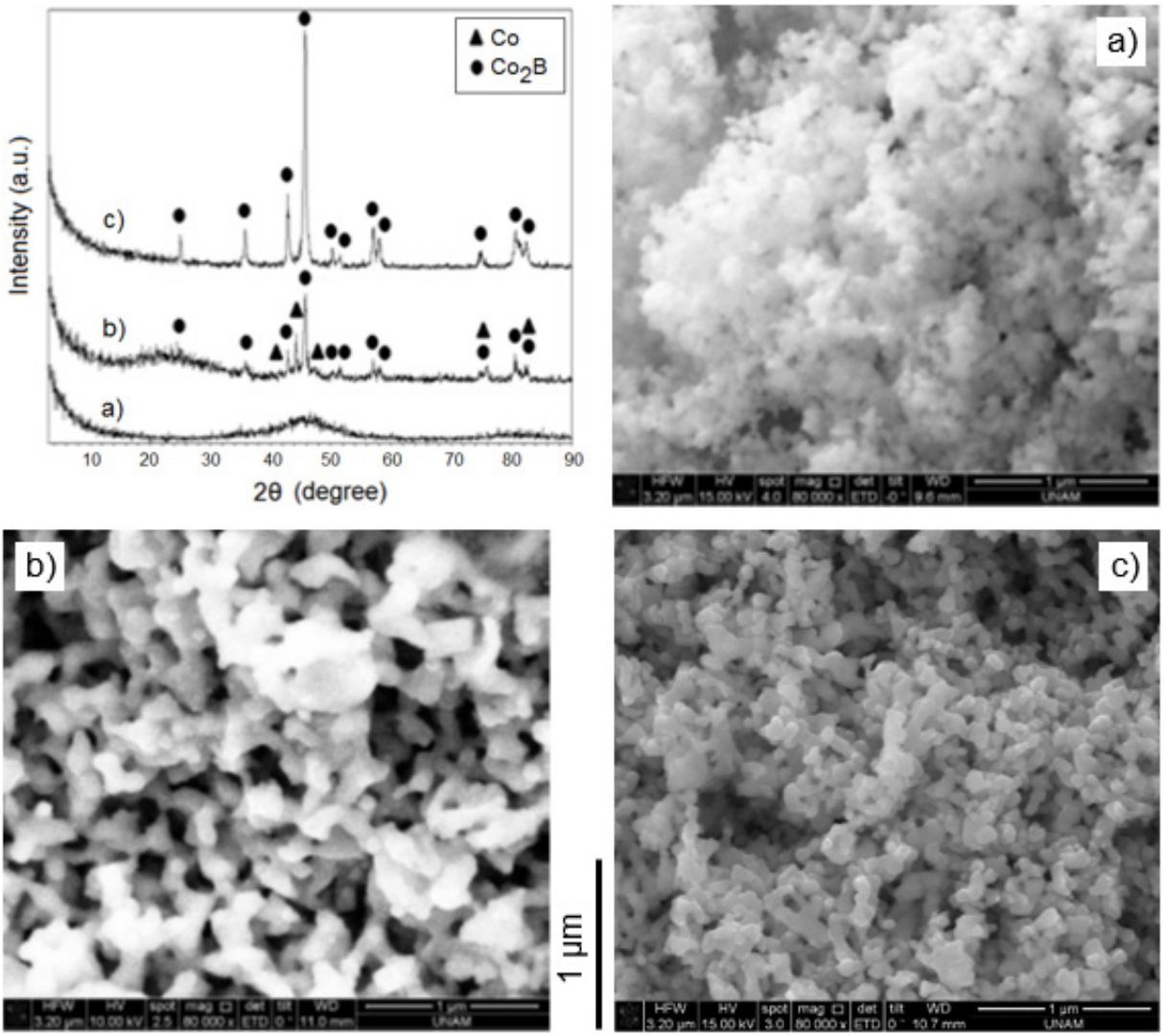

Figure 2. X-Ray diffraction spectra and SEM images of amorphous Co_2B (a), crystalline Co-Co_2B calcined under air (b), crystalline Co_2B calcined under Ar (c)

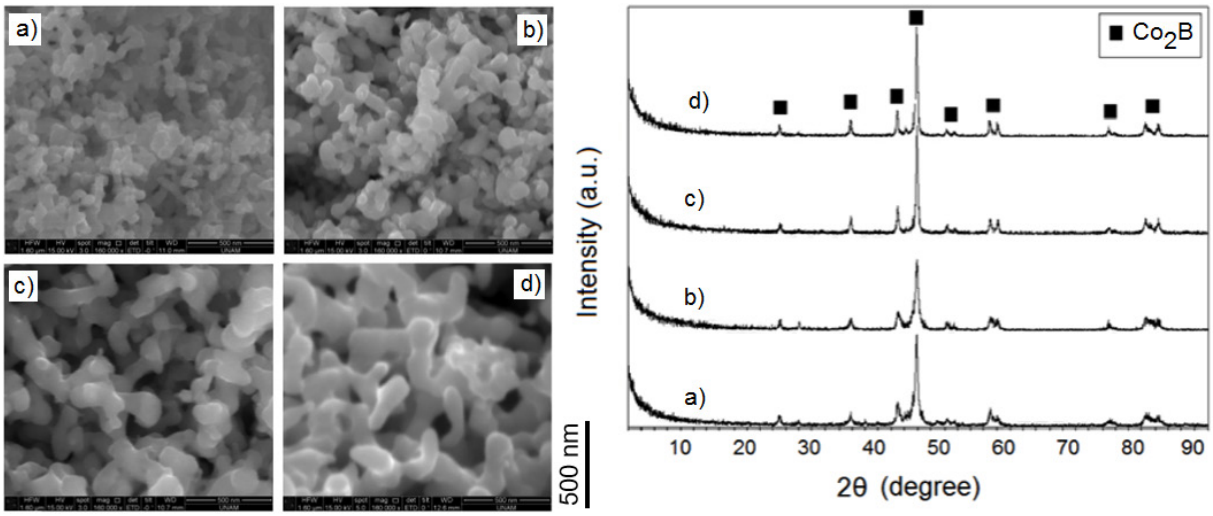

Figure 3. SEM images and X-ray diffraction spectra of cobalt boride particles obtained with different reaction times. (Reaction time (min): (a) 3, (b) 12, (c) 60, (d) 120; $CoCl_2$ concentration:25.0 mM; $NaBH_4$ concentration:59.50 mM, Temperature: +4^oC; Stirring rate:400 rpm; Ar atmosphere)

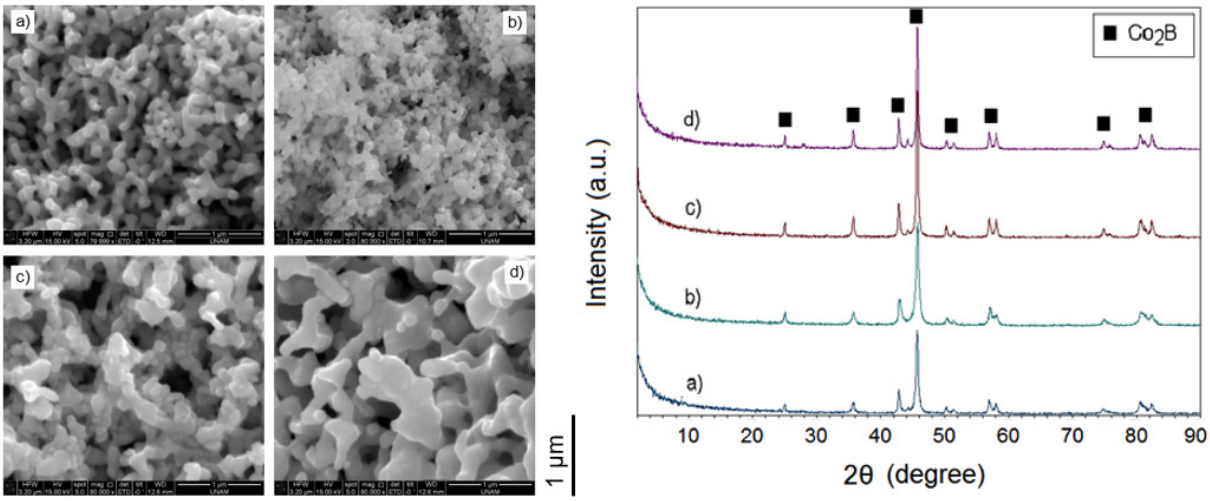

Figure 4. SEM images and X-ray diffraction spectra of cobalt boride particles obtained with different $CoCl_2$ initial concentrations. ($CoCl_2$ concentration (mM): (a) 12.6, (b) 25.0, (c) 50.1 (d) 100.1, $NaBH_4/CoCl_2$ molar ratio: 2.4, Reaction time: 12 min, Temperature: +4^oC, Stirring rate: 400 rpm, Ar atmosphere.)

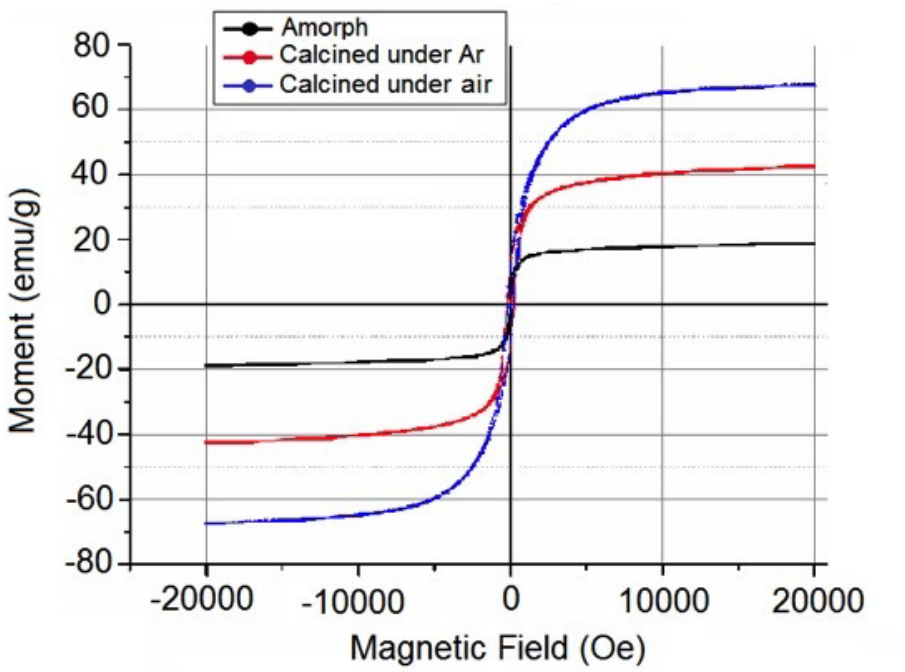

Figure 5. Magnetization curves of the of cobalt boride nanoparticles calcined under different conditions

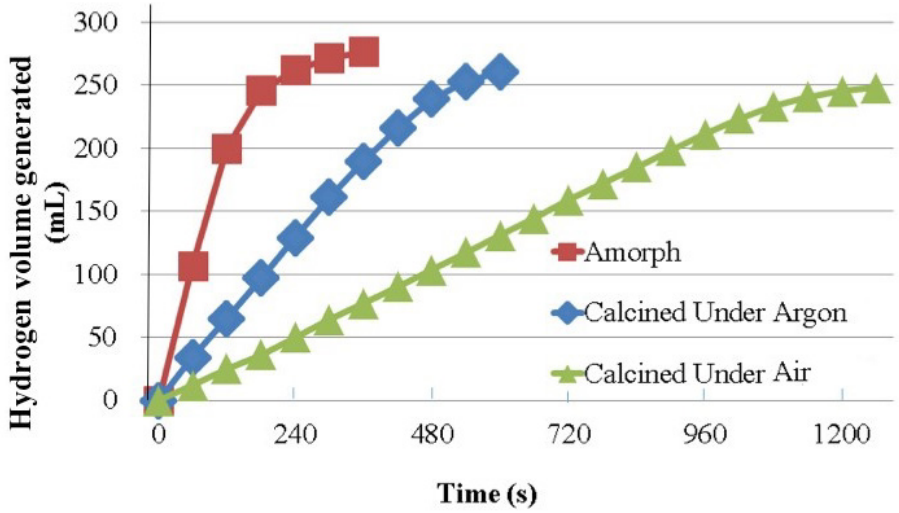

Figure 6. The variation of hydrogen volume with the time by using cobalt boride nanoparticles/nanocylinders obtained with different calcination conditions as catalyst in the hydrolysis of $NaBH_4$. Co_2B concentration: 10 mg/mL, Initial $NaBH_4$ concentration: 263.1 mM (~1 % w/w), NaOH concentration: 250 mM, Room temperature.

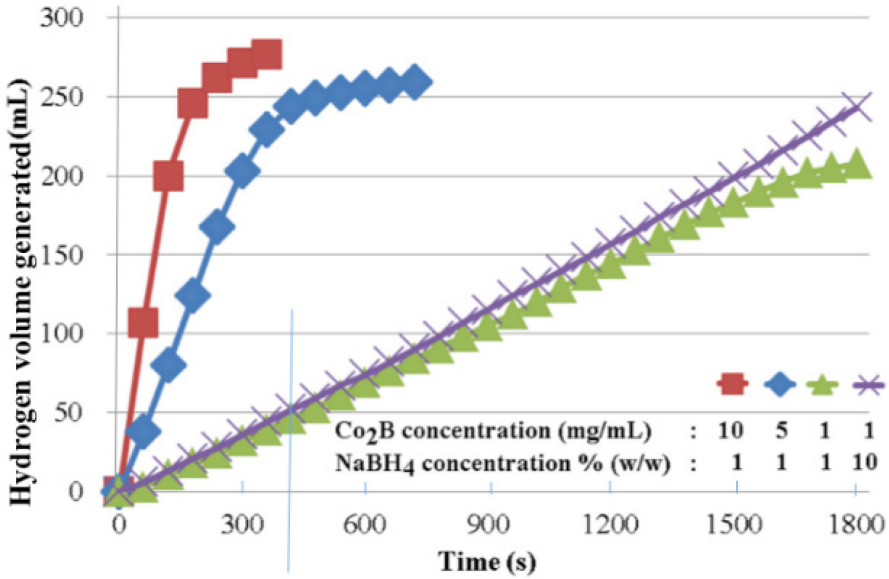

Figure 7. The variation of H_2 volume with the time by using different concentrations of cobalt boride nanoparticles/nanocylinders and different initial $NaBH_4$ concentrations in the hydrolysis of $NaBH_4$. NaOH concentration: 250 mM, Room temperature.

Tables

Table 1. Hydrogen generation rates obtained with the crystalline and amorphous Co_2B samples at different conditions.

Run code	Catalyst	$NaBH_4$ concentration (% w/w)	Co_2B concentration (mg/mL solution)	H_2 generation rate (mLH_2/gcat.min)
C1	Crystalline Co_2B (Calcined under air)	1.0	10.0	132
C2	Crystalline Co_2B (Calcined under Ar)	1.0	10.0	338
A1	Amorphous Co_2B (Dried in vacuo)	1.0	10.0	1110
A2	Amorphous Co_2B (Dried in vacuo)	1.0	5.0	859
A3	Amorphous Co_2B (Dried in vacuo)	1.0	1.0	675
A4	Amorphous Co_2B (Dried in vacuo)	10.0	1.0	757
A5	Amorphous Co_2B (Dried in vacuo)	20.0	1.0	774

Table 2. The properties of hydrogen generation rates of catalysts containing Co_2B phase

Properties of Catalyst	**Particle form**	**Temperature (°C)**	**$NaBH_4$ conc. (% w/w)**	**H_2 generation rate (mL H_2/g cat.min)**	**Reference**
Calcined-crystalline catalyst containing Co and Co_2B	powder	15	2	2970	[25]
Amorphous cobalt boride catalyst in the form of Co-B alloy	irregular nanoparticles	20	20	900	[26]
Calcined cobalt boride catalyst containing Co[c] on Ni foam	irregular nanoparticles and nanocylinders	20	25	7300[a]/1900[b]	[27]
Calcined-crystalline catalyst particles containing Co, Co_3O_4, CoB, Co_2B and Co_3B	irregular	20	20	2400	[28]
Amorphous cobalt boride catalyst containing cobalt oxide	Irregular nanoparticles	20	1	1800	[30]
Mesoporous-amorphous cobalt boride catalyst	irregular nanoparticles	RT	ca 0.1	3350	[31]
Amorphous cobalt boride catalyst	irregular nanoparticles	***18***	***10***	***1110***	***This study***

a: Cobalt boride nanoparticles calcined at 250°C, b: Cobalt boride nanocylinders calcined at 500°C, c: metallic Co was seen in the calcinations performed at the temperatures higher than 300°C.